ORGANOMETALLICS

Article

Cite This: *Organometallics* 2018, 37, 891−899

Half-Sandwich Arene Ruthenium(II) and Osmium(II) Thiosemicarbazone Complexes: Solution Behavior and Antiproliferative Activity

Anna Gatti,[†,‡] Abraha Habtemariam,[‡] Isolda Romero-Canelón,[‡,§] Ji-Inn Song,[‡] Bindy Heer,[‡] Guy J. Clarkson,[‡] Dominga Rogolino,[†] Peter J. Sadler,*[,‡] and Mauro Carcelli*[,†]

[†]Dipartimento di Scienze Chimiche, della Vita e della Sostenibilità Ambientale and CIRCMSB (Consorzio Interuniversitario di Ricerca in Chimica dei Metalli nei Sistemi Biologici), University of Parma, Parco Area delle Scienze 11/A, 43124 Parma, Italy

[‡]Department of Chemistry, University of Warwick, Gibbet Hill Road, Coventry CV4 7AL, United Kingdom

[§]School of Pharmacy, University of Birmingham, Birmingham B15 2TT, United Kingdom

Supporting Information

ABSTRACT: We report the synthesis, characterization, and antiproliferative activity of organo-osmium(II) and organo-ruthenium(II) half-sandwich complexes [(η^6-*p*-cym)Os(L)Cl]-Cl (**1** and **2**) and [(η^6-*p*-cym)Ru(L)Cl]Cl (**3** and **4**), where L = *N*-(2-hydroxy)-3-methoxybenzylidenethiosemicarbazide (**L1**) or *N*-(2,3-dihydroxybenzylidene)-3-phenylthiosemicarbazide (**L2**), respectively. X-ray crystallography showed that all four complexes possess half-sandwich pseudo-octahedral "three-legged piano-stool" structures, with a neutral N,S-chelating thiosemicarbazone ligand and a terminal chloride occupying three coordination positions. In methanol, *E*/*Z* isomerization of the coordinated thiosemicarbazone ligand was observed, while in an aprotic solvent like acetone, partial dissociation of the ligand occurs, reaching complete displacement in a more coordinating solvent like DMSO. In general, the complexes exhibited good activity toward A2780 ovarian, A2780Cis cisplatin-resistant ovarian, A549 lung, HCT116 colon, and PC3 prostate cancer cells. In particular, ruthenium complex **3** does not present cross-resistance with the clinical drug cisplatin in the A2780 human ovarian cancer cell line. The complexes were more active than the free thiosemicarbazone ligands, especially in A549 and HCT116 cells with potency improvements of up to 20-fold between organic ligand **L1** and ruthenium complex **1**.

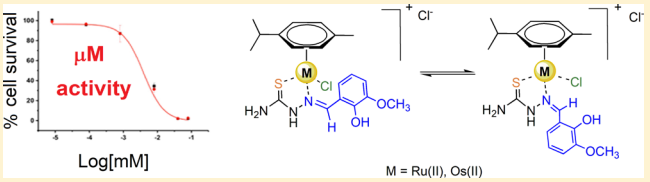

INTRODUCTION

The discovery of highly efficient anticancer drugs with increased selectivity and less toxic side effects is an area of intense research in bioinorganic chemistry.[1] Thiosemicarbazones (TSCs) and their metal complexes display a wide spectrum of biological activities,[2−5] in particular they possess anticancer, antibacterial, and antiviral properties.[6−8] A variety of cellular mechanisms of action appears to be involved in the activity of this class of ligands,[9] including the inhibition of cellular iron uptake by transferrin,[10−12] the mobilization of iron from cells,[6−8] the inhibition of ribonucleotide reductase activity,[13−15] the up-regulation of the metastasis suppressor protein, *N*-myc downstream regulated gene I,[16,17] and the formation of redox active metal complexes that produce reactive oxygen species.[11,18−20] Moreover, various studies[21] have demonstrated that the biological properties of TSC ligands can be modified and improved upon binding to transition metal ions.[6,22] Metal coordination presents an opportunity to improve synergistically the efficacy of a biologically active organic scaffold[23] such as lipophilicity, which influences cell permeability.[24] Diversity arises from not only the choice of the metal itself and its oxidation state but also from the type and number of coordinated ligands, as well as the coordination geometry of the complex.[23]

Metal complexes of TSCs are playing a promising role in anticancer research, as is evident from the number of recent publications.[8,25−27] Platinum drugs are still widely used to treat cancer,[5,28] but their therapeutic use can be limited by intrinsic or acquired resistance and by the occurrence of numerous deleterious side effects.[29,30] It is imperative, therefore, to develop new and more effective drugs. Ruthenium, a second row transition metal, continues to attract much attention,[31,32] as its complexes have long been known to be well-suited for biological applications.[33,34] Organometallic Ru(II) complexes with half-sandwich structure have demonstrated antiproliferative potential,[35] and there are numerous possibilities to modulate their biological and pharmacological properties by the appropriate choice of the ligands.[11,36] In particular, the presence of a chelating ligand offers structural stability and the opportunity to tune the electronic and steric features of the complex.[37] Additional features to be considered include water solubility and air stability.[37,38] The biological activity of osmium compounds has been much less explored, perhaps because of the reputation of osmium (as osmium tetroxide) as being highly toxic.[39] Nevertheless, several half-sandwich piano-stool

Received: December 7, 2017
Published: February 20, 2018

DOI: 10.1021/acs.organomet.7b00875
Organometallics 2018, 37, 891−899

osmium(II) complexes have exhibited promising *in vitro* activity and no cisplatin cross-resistance.[40−42] Investigations of osmium complexes as alternatives to ruthenium-based anticancer agents have resulted in structurally diverse libraries of osmium complexes with different oxidation states and nuclearity.[43−46]

Organometallic chemistry offers a potentially rich field for biological and medicinal application;[47] however, lack of understanding of the aqueous chemistry of the organometallic complexes has emerged as a major obstacle for further developments. This is particularly true for osmium(II) arene complexes.[48] Third row transition metals are more inert than those of the first and second row. For example, aquation of Pt(II) chlorido complexes often occurs up to 10^4 times more slowly compared to the lighter congener Pd(II), and similarly, organo-Os(II) complexes react typically 100 times more slowly than Ru(II).[49−51] However, reports on ruthenium arene complexes have shown that their aqueous reactivity is highly dependent on the nature of the coordinated ligands, as well as the arene, rather than on the metal and its oxidation state alone.[52,53]

The aim of the present study is to investigate the reactivity in solution and the antiproliferative activity toward cancer cells of two Os(II) complexes [(η^6-*p*-cym)Os(L)Cl]Cl (**1** and **2**) and two analogous Ru(II) complexes [(η^6-*p*-cym)Ru(L)Cl]Cl (**3** and **4**), where L = *N*-(2-hydroxy)-3-methoxybenzylidenethiosemicarbazide (**L1**) or *N*-(2,3-dihydroxybenzylidene)-3-phenylthiosemicarbazide (**L2**), respectively (Figure 1). This type of

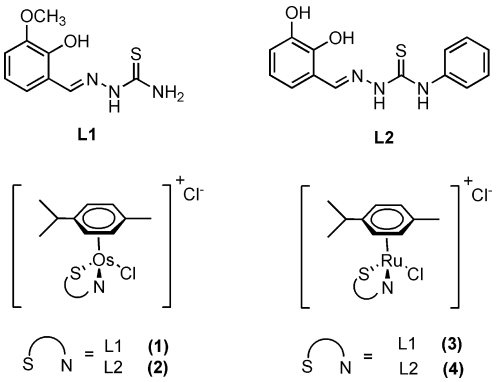

Figure 1. Schematic representation of ligands **L1** and **L2** and corresponding osmium(II) and ruthenium(II) complexes **1**−**4**.

ligands, which could in principle be tridentate, can confer solution stability on their metal complexes; moreover they have shown interesting cytotoxic properties[54] and could offer synergic antitumor activity. Different substituents were considered for ligands **L1** and **L2** on both the phenyl ring and at the N(3) nitrogen, since this can modulate lipophilicity and/or complex−substrate interactions. The solution behavior of complexes **1**−**4** was studied both in a protic solvents such as methanol or water/DMSO mixture and in coordinating aprotic solvents like acetone, DMSO and DMF. The antiproliferative activity of **1**−**4** was evaluated for A2780 human ovarian carcinoma and its cisplatin resistant variant A2780Cis, A549 lung, HCT116 colon, and PC3 prostate tumor cell lines.

RESULTS AND DISCUSSION

Synthesis and Characterization of the Complexes. Ligands *N*-(2-hydroxy)-3-methoxybenzylidenethiosemicarbazide (**L1**) and *N*-(2,3-dihydroxybenzylidene)-3-phenylthiosemicarbazide (**L2**) were synthesized according to previously reported procedures.[54,55] The reactions between [(η^6-*p*-cym)-MCl_2]$_2$ (M = Os and Ru) and the corresponding thiosemicarbazone ligands were carried out in a mixture of dry CH_3OH and CH_2Cl_2 at ambient temperature and led to the isolation of pseudo-octahedral complexes **1**−**4** of general formula [(η^6-*p*-cym)M(L)Cl]Cl in good yields. The identity of the complexes was verified by ^{1}H NMR spectroscopy and ESI-MS spectrometry, and their structures were confirmed by single crystal X-ray crystallography. In all cases, the metal coordinates to a chloride ion, a η^6-*p*-cymene ring and a *NS*-bidentate thiosemicarbazone chelating ligand. One chloride is present as the counterion (Figure 1).

X-ray Crystallographic Studies. Crystals suitable for X-ray diffraction analysis were obtained by slow evaporation of saturated solutions in methanol for compounds **1** and **3** and in acetone for compounds **2** and **4**. The crystal structures and atomic numbering schemes for [(η^6-*p*-cym)Os(**L1**)Cl]Cl (**1**), [(η^6-*p*-cym)Os(**L2**)Cl]Cl·$(CH_3)_2CO$ (**2**·$(CH_3)_2CO$), [(η^6-*p*-cym)Ru(**L1**)Cl]Cl (**3**), and [(η^6-*p*-cym)Ru(**L2**)Cl]Cl·$(CH_3)_2CO$ (**4**·$(CH_3)_2CO$) are shown in Figure 2. Selected bond lengths and angles are listed in Table 1, other crystallographic data are reported in Table S1. Complexes **1** and **3** crystallize in the orthorhombic system with the chiral space group $P2_12_12_1$, while complexes **2** and **4** crystallize in triclinic system with centrosymmetric space group $P\bar{1}$. Both **2** and **4** crystallize with an acetone solvent molecule. The complexes adopt the expected half-sandwich pseudo-octahedral "three-legged piano-stool" geometry with η^6-*p*-cymene as the seat and the neutral N,S-chelating TSC ligand and a terminal chloride as the three legs. The positive charge of the complex is balanced by a chloride counterion. It is notable that in all the complexes, the ligand is present as the *E* isomer.

In **1** and **3**, the uncoordinated chloride anion forms a NH···Cl hydrogen bond of 3.034(4) Å and 175.1° for **1**, and 3.031(3) and 176.7° for **3**. In **2** and **4**, a similar H-bond occurs between the uncoordinated chloride and the 3-OH group of the aromatic ring with a bond distance OH···Cl of 3.0651(16) Å and 169.0° for **2**, and 3.0605(9) Å and 168.7° for **4**. The thiosemicarbazone ligands bind to the metal center through the imine nitrogen and the thione sulfur forming a five member chelate ring with an angle of 82° for N−Ru−S, indicating a distortion from a regular octahedron, in analogy with similar Ru−arene thiosemicarbazone complexes.[56] The length of the S−C bond (∼1.69 Å) is in accord with a double bond nature; in the free ligands, it is ∼1.69−1.70 Å.[57−59]

It is worth noting that in some osmium(II) and ruthenium(II) arene complexes the potentially NNO tridentate hydrazone ligands behave as NN bidentate ligands. It has been highlighted that the ligands are not flexible enough to occupy a facial arrangement in the complex and are therefore bidentate.[60] An analogous situation could occur with **L1** and **L2** that can span the three facial coordination sites of the metal only with difficulty. Interestingly, these hydrazone ligands were found in both *E* and *Z* configuration upon complexation with Ru(II) and Os(II). The dihedral angles between the aromatic ring plane and the thiosemicarbazones are around 70° in complexes **1** and **3** and about 78° in **2** and **4**. Usually, this type of ligand adopts a flat conformation:[58,59,61] In our structures, the lack of coplanarity is related to metal coordination. In the crystal structures of **1**−**4**, the same T-shaped edge-to-face stacking π-interactions, between one of the hydrogens of the *p*-cymene ring and the π electron density of the aromatic ring of the

DOI: 10.1021/acs.organomet.7b00875
Organometallics 2018, 37, 891−899

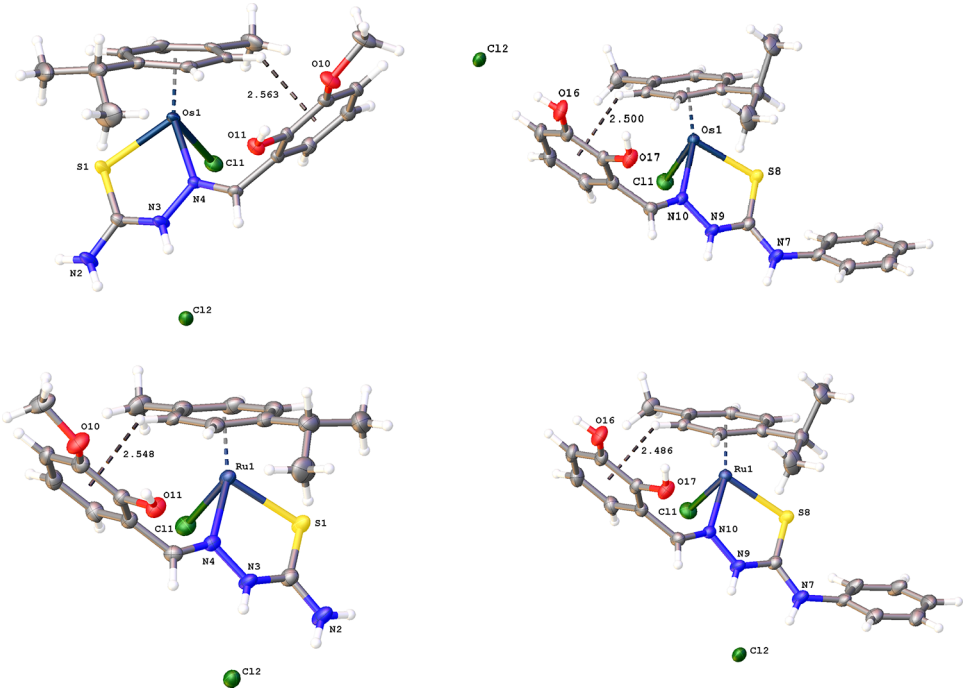

Figure 2. X-ray crystal structures of complexes **1**−**4** with thermal ellipsoids drawn at 50% probability. Hydrogens are drawn as fixed-size spheres of 0.11 Å radius and solvent molecules have been omitted for clarity. The edge-to-face stacking between one of the hydrogens of the *p*-cymene ring and an aromatic ring of the thiosemicarbazone ligands is indicated.

Table 1. Selected Bond Lengths (Å) and Angles (deg) for Complexes 1−4

		bond distance (Å)		bond angle (deg)
	Os1−Cl1	2.4113(12)	S1−Os1−Cl1	86.52(4)
	Os1−S1	2.3551(13)	N4−Os1−Cl1	81.63(10)
1	Os1−N4	2.118(4)	N4−Os1−S1	81.63(11)
	S1−C2	1.695(5)		
	H14−CE1	2.563		
	Os1−Cl1	2.4030(5)	S8−Os1−Cl1	87.81(2)
	Os1−S8	2.3527(5)	N4−Os1−Cl1	83.44(5)
2·$(CH_3)_2CO$	Os1−N10	2.1227(17)	N10−Os1−S8	81.79(5)
	S8−C8	1.693(2)		
	H21−CE1	2.500		
	Ru1−Cl1	2.4046(11)	S1−Ru1−Cl1	86.90(4)
	Ru1−S1	2.3501(10)	N4−Ru1−Cl1	83.06(9)
3	Ru1−N4	2.125(3)	N4−Ru1−S1	81.95(10)
	S1−C2	1.695(4)		
	H14−CE1	2.548		
	Ru1−Cl1	2.3993(3)	S8−Ru1−Cl1	88.338(11)
	Ru1−S8	2.3508(3)	N10−Ru1−Cl1	84.77(3)
4·$(CH_3)_2CO$	Ru1−N10	2.1256(9)	N10−Ru1−S8	81.94(3)
	S8−C8	1.6923(12)		
	H21−CE1	2.486		

thiosemicarbazone ligands, are observed (distances from 2.50 to 2.86 Å, Figure 2).

Solution Studies. ^{1}H NMR studies were used to investigate the stability of the four complexes in various solvents. ^{1}H NMR spectra of **1**−**4** were first recorded in MeOD-d_4, due to their low solubility in chlorinated solvents such as chloroform or dichloromethane. For all the metal complexes, the spectra displayed just one set of signals, corresponding to the *E* isomer of the bidentate ligand coordinated to the metal center, the isomer in the crystallized complexes. The aromatic protons of the thiosemicarbazone ligands displayed peaks between 6.5 and 8.2 ppm, and the iminic protons displayed peaks between 8.7 and 8.9 ppm, as expected for the ligand in the *E* form.[55,62] The complexes contain chiral metal centers and in the ^{1}H NMR spectra recorded at 298 K a doublet is present for each *p*-cymene proton in the range 4.90−5.90 ppm; the isopropyl methyl groups appear as two doublets at 1.1 and 1.2 ppm. The resonance of one proton of the *p*-cymene ring displays a marked high-field shift in comparison with the other *p*-cymene protons, in particular up to 4.90 ppm for osmium compounds **1** and **2** and 4.87 for ruthenium **3** and **4** (Figure 3). This is likely due to edge-to-face π-interaction between the C−H hydrogen

DOI: 10.1021/acs.organomet.7b00875
Organometallics 2018, 37, 891−899

and the aromatic ring of the TSC ligand in the *E* form, as observed previously in analogous systems.[21,63]

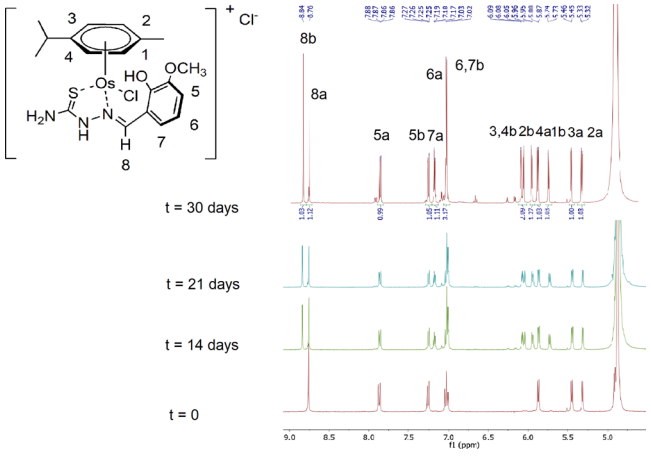

Figure 3. Aromatic region of the time-dependent ^{1}H NMR spectrum of **1** in MeOD-d_4 at T = 298 K followed over 30 days. *E* and *Z* isomers are labeled as *a* and *b* sets, respectively. The percentage of the *Z* isomer (*b* set) increases with time.

The time dependence of the ^{1}H NMR spectra of **1**–**4** (5 mM) in MeOD-d_4 was monitored over 30 days at 298 K, and is illustrated for complex **1** in Figure 3. As shown in Figure 3, a second set of peaks started to appear after 24 h (set *b*) and increased in intensity until a 1:1 ratio for the two species was reached over a period of 21 days. Variable-temperature ^{1}H NMR spectra were recorded from 298 to 323 K over a period of 2 h. The 1:1 ratio of the *a*/*b* peak areas for the two species recorded at t = 30 days did not change over this temperature range (data not shown). NOESY experiments carried out for **1** at t = 30 days, gave evidence that in the *b* set of peaks there is an interaction between the iminic hydrogen of the ligand and one of the aromatic protons of the *p*-cymene (Figure S1); this interaction is absent in the *a* set. A possible explanation for the presence, in solution, of two species (corresponding to set *a* and set *b*) is the establishment of an *E*/*Z* equilibrium for coordinated ligand **L1** (Figure 4). The presence of both the *E* and the *Z* isomers of the ligand coordinated to the metal center would explain the interaction of the iminic proton with the *p*-cymene moiety, observed for set *b* in the NOESY experiment. This interaction is possible only for a *Z* conformation of the ligand and not with the *E* conformation. TSCs are known to undergo *E*/*Z* interconversion not only as free ligands but also upon coordination (for a mechanistic insight see ref 64 and references therein).

The increase in the percentage of Z isomer suggests that the presence of a protic solvent could lead to the formation of a negative charge on the iminic nitrogen and to the rotation around the single bond, resulting in the isomerization and the formation of the *Z* isomer, as proposed in Scheme 1. This mechanism is supported by the ^{1}H NMR spectrum of the crystals of the complexes in methanol. In the X-ray crystal structures of **1** and **3**, obtained from a methanol solution, the ligand is in the *E* conformation, but the ^{1}H NMR spectra of the same crystals recorded in MeOD-d_4 showed the presence of both isomers of the ligands after 24 h, suggesting that the solvent plays a crucial role in the isomerization process. Recently, examples of pentamethylcyclopentadienyl iridium(III) complexes with TSCs ligands that crystallize with the

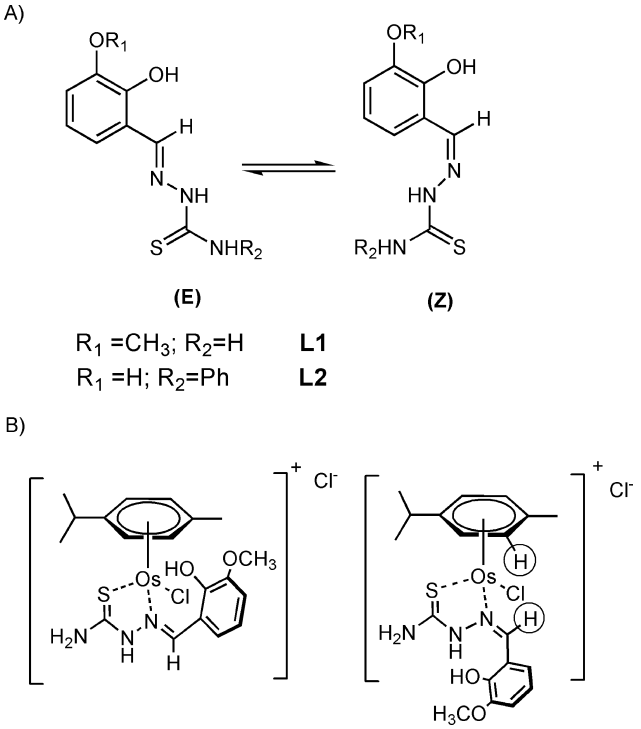

Figure 4. (A) *E*/*Z* interconversion for **L1** and **L2**. (B) Chemical structures of the *E* and *Z* isomers of ligand **L1** in the complex **1**; the interaction between the iminic proton and one proton of the *p*-cymene is depicted by circles.

coordinated ligand either with *E* or *Z* conformation have been reported, confirming the possibility of having both isomers in organometallic complexes.[65]

Analysis of the data provides evidence that the interconversion is slightly faster for the ruthenium compound: at 298 K the *Z* isomer takes 2 weeks to reach the equilibrium with the *E* isomer (1:1 ratio), whereas 3 weeks are required for the osmium complex. The situation is slightly different for complexes **2** and **4**. For these complexes a second set of signals arises over time (1:1 ratio at t = 7 days and 298 K, Figure S2). However, the ^{1}H NMR spectra of these complexes show broad signals in the aromatic region for the *Z* isomer (Figure S2). For complex **4**, for example, at t = 7 days only very broad overlapping signals can be seen (Figure S3). The presence of two hydroxyl groups on the aromatic ring of the coordinated ligand perhaps gives rise to exchange processes or paramagnetic species which broaden signals in the ^{1}H NMR spectra.

Due to the long-time scale of the NMR experiments and the catecholic nature of ligand **L2**, complexes **2** and **4** can be subjected to oxidation. UV–visible spectroscopy was performed in order to verify whether the catechol moiety of **2** is involved in oxidation processes in methanol solution. The development of a stable and strong absorption band of a methanol solution of **2** around 337 nm, related to π–π^* transition of the catechol aromatic ring, was followed over 3 days in air (Figure S4). No changes in the UV–vis spectra were detected, indicating that the catechol moiety is not involved in redox processes. ^{1}H NMR spectra of complexes **1**–**4** were also recorded in an aprotic solvent, acetone. In this case, two different sets of signals were observed immediately after dissolution in acetone-d_6 at 298 K for all the complexes (Figure 5). Comparison with the ^{1}H NMR obtained in MeOD at t = 0 indicates that one set

DOI: 10.1021/acs.organomet.7b00875
Organometallics 2018, 37, 891–899

Scheme 1. Proposed Mechanism for the *E*/*Z* Interconversion Process of the Coordinated Ligand L1 for Metal Complexes 1 and 3 in Methanol

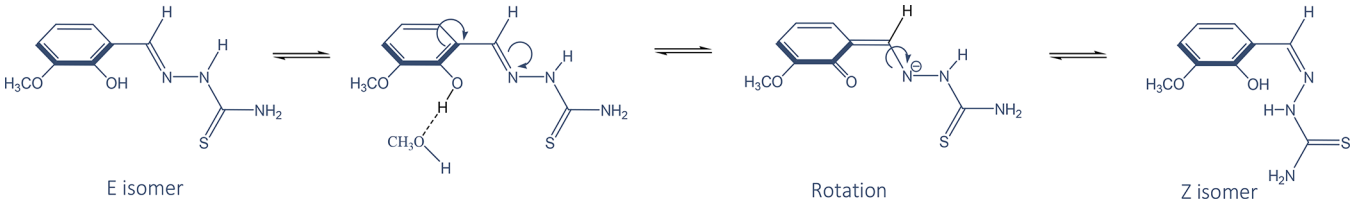

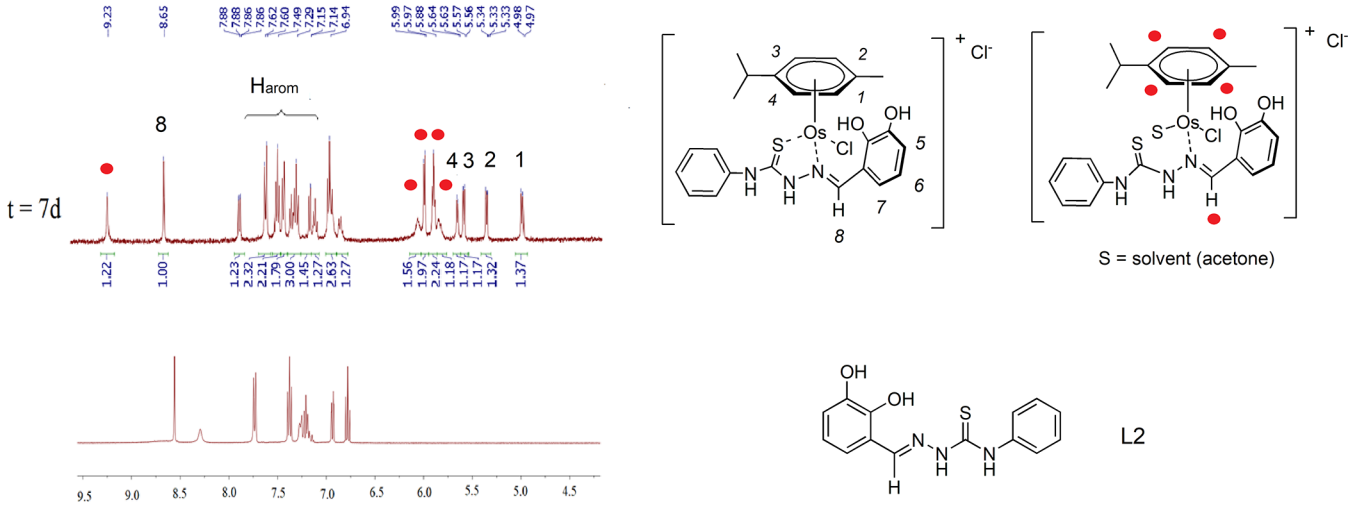

Figure 5. Aromatic region of the ^{1}H NMR spectrum of **2** recorded in acetone-d_6 at 298 K and followed over 7 days. Red circles indicate proton resonances related to the species with a coordinated solvent molecule.

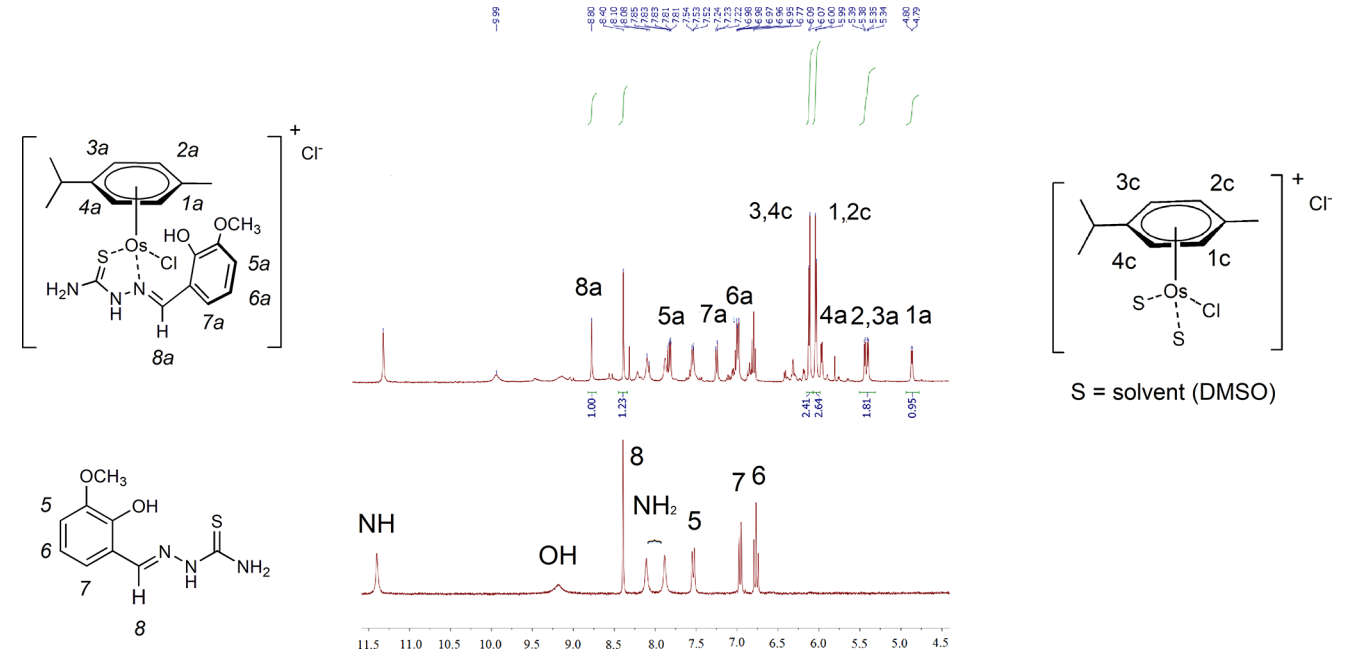

Figure 6. Comparison of the aromatic region of the ^{1}H NMR of complex **1** (upper spectrum) and that of the corresponding free ligand **L1** (lower spectrum) in DMSO-d_6 at t = 0 and 298 K.

of signals is related to the parent organometallic compound, as shown in Figure 5 for compound **2**. The presence of free ligand was excluded by comparison with the ^{1}H NMR spectrum of **L2** recorded in acetone-d_6. It is notable that the ^{1}H NMR spectra change with time at 298 K. As shown in Figure 5, both a shift and a modification of the pattern of the signals is observed over 2 days. After this time the two sets of signals did not change their ratio (ca. 1:1.2). Probably, the second set of signals is due to a species containing a coordinated solvent molecule (Figure 5).

Due to the limited aqueous solubility of the metal complexes, antiproliferative cell assays were performed using stock

DOI: 10.1021/acs.organomet.7b00875
Organometallics 2018, 37, 891−899

Table 2. IC_{50} Values (μM) for L1 and L2 and Related Metal Complexes 1−4 towards Human Ovarian (A2780), Cisplatin-Resistant Ovarian (A2780Cis), Lung (A549), Colon (HCT116), and Prostate (PC3) Cancer Cell Lines[a]

	cell lines IC_{50} (μM)					resistance factors
compound	A2780	A2780Cis	A549	HCT116	PC3	A2780Cis/A2780
L1	0.85 ± 0.03	0.12 ± 0.02	42 ± 2	30.6 ± 0.5	6.1 ± 0.1	0.14
L2	0.27 ± 0.02	1.23 ± 0.08	23 ± 1	33 ± 5	4.6 ± 0.2	4.55
1	1.60 ± 0.02	6.6 ± 0.9	2.4 ± 0.2	24 ± 2	21 ± 1	4.12
2	0.75 ± 0.08	7.2 ± 0.1	17 ± 1	2.7 ± 0.2	1.60 ± 0.08	9.60
3	4.2 ± 0.3	5.6 ± 0.8		10.5 ± 0.3	19 ± 1	1.33
4	0.36 ± 0.03	1.25 ± 0.06		1.64 ± 0.08	1.38 ± 0.04	3.47
CDDP	1.2 ± 0.2	13.5 ± 0.3	3.1 ± 0.2	5.2 ± 0.1	9.8 ± 0.4	11.25

[a]Clinical drug cisplatin (CDDP) is used as positive control.

solutions prepared by dissolution of the compound in DMSO followed by dilution with water (final concentration of DMSO 0.5%). The hydrolysis processes are of interest as indicators of the stability of the pro-drug under such biological testing conditions; therefore, the solution behavior of **1**−**4** was investigated also in DMSO-d_6. In the ^{1}H NMR spectra of **1** and **3** in DMSO-d_6 recorded at 298 K, three different sets of signals were observed. A comparison with the ^{1}H NMR spectrum of **L1** obtained in the same solvent confirmed the presence of free ligand in a 1:1 ratio versus the metal complex (Figure 6). The two doublets observed at 6.08 and 6.00 ppm can be assigned to a complex of the type [Os(η^6-*p*-cym)(DMSO)$_2$Cl]Cl, in a 1:1 ratio with parent organometallic complex **1** and free ligand **L1**. As recently pointed out in the literature, such a pattern of signals frequently arises after displacement of the organic ligand in [Ru(η^6-*p*-cym)(**L**)Cl$_2$] complexes.[66] Ligand dissociation was apparent visually; addition of DMSO to the orange powder of **1** leads to an orange solution that became green as dissociation proceeded.

Complexes **2** and **4** in DMSO-d_6 gave a complex pattern of ^{1}H NMR signals. Comparison with the spectrum of **2** in MeOD at t = 0 indicates that the major set of signals is related to parent compound **2**. However, other sets of signals of lower intensity were observed (Figure S5). Both sets of signals for free ligand **L2** and the [Os(η^6-*p*-cym)(DMSO)$_2$Cl]Cl species, each accounted for about 10% of the major set. In case of **2** and **4** in DMSO, however, a further set of signals, corresponding to about 25% of the major set, arises in the ^{1}H NMR spectrum. A possible explanation for this set of signals is the presence of a monosolvated species of the type [Os(η^6-*p*-cym)(DMSO)(**L**)-Cl]Cl (Figure S5).

To determine whether the degradation process correlates with the concentration of DMSO, the analysis was performed using a solution of D$_2$O−(10%)DMSO, monitored for 24 h to mimic the biological test conditions. The ^{1}H NMR spectra of the solutions of **1**−**4** displayed in all cases broad signals, with complicated splitting patterns, indicating the presence of several dissociation equilibria in solution. This behavior prevented the use of DMSO in biological tests; therefore, the possibility of preparing stock solutions of the compounds in DMF was investigated. In this case, all complexes **1**−**4** presented a unique set of signals, stable over 7 days at 298 K (Figure S6).

Anticancer Activity. The antiproliferative activity of ligands **L1** and **L2** and of the related osmium and ruthenium complexes **1**−**4** toward A549 lung, A2780 ovarian, HCT116 colon, and PC3 prostate human cancer cells lines was investigated. All experiments included untreated negative controls and cells treated with the clinical drug cisplatin (CDDP) as positive control. The anticancer activity of the organometallic complexes was investigated by performing dose−response studies in the various cell lines (Figure S7). A stock solution of each compound was prepared in cell culture medium with DMF to aid solubilization. IC_{50} values (concentrations which caused 50% of cell growth inhibition) were determined as duplicates of triplicates in two independent sets of experiments and are reported in Table 2. Importantly, all experiments designed to determine the antiproliferative activity of the complexes included three set of controls (negative, vehicle, and positive). The cell survival in the negative controls and the vehicle controls were compared, and in all cases, the differences were not statistically significant to 99%. This indicates that the DMF in the sample solutions of complexes **1**−**4** is not toxic and does not interfere with the measurements. Hence, the effects on cell survival observed arise only from the activity of the ligands or the metal-based complexes.

Both thiosemicarbazones **L1** and **L2** are highly potent toward ovarian cell lines A2780 and A2780Cis. **L1** in particular exhibits IC_{50} values of 0.85 and 0.12 μM, respectively. Ligand **L2** shows submicromolar activity in A2780 cells (0.27 μM) and low micromolar potency in A2780Cis (1.23 μM). Although the metal complexes are less active than their corresponding ligands, they show IC_{50} values of the same order of magnitude as that of CDDP in the parental cell line and improved resistant factors. Resistance factors, calculated as the ratio between the antiproliferative activity in the parental cell line and its resistant derivative, give an indication of whether the cellular mechanisms of resistance to CDDP are involved in the mechanism of action of the novel metal complexes. It has been proposed that the underlying resistance associated with A2780Cis involves a 2-fold more efficient efflux of the platinum drug and a consequent reduction in cellular accumulation as compared to the parental A2780, as well as an increase in DNA repair mechanisms.[67] The corresponding resistance factor for CDDP is 11.25. Complexes **3** and **4** are particularly promising for overcoming CDDP resistance as they have the lowest factors of 1.33 and 3.4, respectively, highlighting the importance of the substituents in the chelating ligands and in particular the incorporation of a phenyl ring at the N(3) of the thiosemicarbazone, when compared to −NH$_2$. For the A549 lung and HCT116 colon cancer cells, there is an improvement in the activity of metal complexes compared to their corresponding ligands, with thiosemicarbazones **L1** and **L2** exhibiting an order of magnitude higher IC_{50} concentrations than the clinical drug CDDP. It is important to highlight the 17-fold improvement in potency between **L1** and its osmium complex **1** increasing from 42 to 2.4 μM in A549 cells, as well as the 12-fold increase in potency between **L2** (33 μM) and osmium complex **2** (2.7 μM) and 20-fold compared to

DOI: 10.1021/acs.organomet.7b00875
Organometallics 2018, 37, 891−899

ruthenium complex **4** (1.64 μM) in the HCT116 colon cell line. The prostate cancer cell line PC3 shows mixed results with increments in potency for complexes **2** and **4** derived from **L2** but reduction in anticancer activity for complexes **1** and **3** derived from **L1**. The former are more active than CDDP in this cell line. The observed trends in the anticancer activity, across all cell lines and all compounds, point toward complexes with ligand **L2** being more potent than those which bear ligand **L1**, and within this, ruthenium complex **4** has a more potent activity compared to the osmium analogue. This highlights that the anticancer activity of the complexes is not only the result of the metal center *per se*, but also of the nature of the substituents on the thiosemicarbazone ligands.

CONCLUSIONS

Two new osmium(II) and two ruthenium(II) half-sandwich complexes $[(\eta^6\text{-}p\text{-cym})M(L)Cl]Cl$ containing a thiosemicarbazone ligand (L) were synthesized and characterized by ^{1}H NMR, ESI-MS spectrometry and single crystal X-ray crystallography. Complexes **1**−**4** are structurally very similar and characterized by a distorted octahedral geometry. In the crystal structures, the *E* configuration of the thiosemicarbazone ligand was evident.

In a protic solvent, such as methanol, an interconversion takes place and peaks for both *E* and *Z* isomers of the ligand appear in the ^{1}H NMR spectrum. The conformational change in the ligand is probably promoted by the interaction of the solvent with the acidic proton of the aromatic ring. When the complexes were dissolved in the nonprotic, coordinating acetone or in DMSO, solvation reactions prevailed. On the contrary, in DMF solution, the complexes remained stable. Hence, DMF (5%) and not DMSO was used to aid solubility for cancer cell screening. Promising results were obtained, particularly toward HCT116 colon cancer cells, in which the metal complexes are up to 20-fold more potent than corresponding free ligand **L2**. Ruthenium complex **3** shows promising anticancer activity, and the possibility to overcome CDDP resistance as demonstrated by the data for A2780 ovarian cancer cells and its derived CDDP-resistant cell line A2780Cis. In fact all complexes showed lower resistance factors than the clinical drug cisplatin. Future work will aim at optimizing the pharmacological profiles of these complexes, especially to increase stability under biological testing conditions.

EXPERIMENTAL SECTION

Materials. All commercial reagents were used as received. 2-Hydroxy-3-methoxybenzaldehyde, 2,3-dihydroxybenzaldehyde, thiosemicarbazide, and 4-phenylthiosemicarbazide were purchased from Sigma-Aldrich; $OsCl_3{\cdot}nH_2O$ and $RuCl_3{\cdot}nH_2O$ were from Alfa Aesar. All reactions were performed under an inert atmosphere of nitrogen using standard Schlenk line techniques, and all glassware was oven-dried (120 °C) overnight. Dry solvents were purchased from Sigma-Aldrich and stored under nitrogen. $[(\eta^6\text{-}p\text{-cym})OsCl_2]_2$ and $[(\eta^6\text{-}p\text{-cym})RuCl_2]_2$ were synthesized according to literature procedures.[49,68]

Cell Culture. Cell lines used in this work included A2780 human ovarian carcinoma and its cisplatin-resistant variant A2780Cis, A549 human caucasian lung carcinoma, HCT116 human colon carcinoma, and PC3 human prostate carcinoma. They were all obtained from the European Collection of Cell Cultures (ECACC), used between passages 5 and 18 and were grown in Roswell Park Memorial Institute medium (RPMI-1640) supplemented with 10% (v/v) of fetal calf serum, 1% (v/v) of 2 mM glutamine and 1% (v/v) penicillin/streptomycin. They were grown as adherent monolayers at 310 K in a 5% CO_2 humidified atmosphere and passaged at ca. 70−80% confluence.

***In Vitro* Growth Inhibition Assay.** Briefly, 5000 cells were seeded per well in 96-well plates. The cells were preincubated in drug-free media at 310 K for 48 h before adding different concentrations of the compounds to be tested. A stock solution of the metal complex was first prepared in 5% DMF (v/v) and a mixture 0.9% saline and medium (1:1) (v/v) following serial dilutions in RPMI-1640. The drug exposure period was 24 h. After this, supernatants were removed by suction, and each well was washed with PBS. A further 72 h was allowed for the cells to recover in drug-free medium at 310 K. The SRB assay was used to determine cell viability. Absorbance measurements of the solubilized dye allowed the determination of viable treated cells compared to untreated controls. IC_{50} values (concentrations which caused 50% of cell growth inhibition) were determined as duplicates of triplicates in two independent sets of experiments and their standard deviations were calculated. All experiments included three sets of controls: (a) negative controls, in which cells were kept untreated, (b) vehicle controls, in which cells were exposed to medium with vehicle only (in this case DMF, at the highest concentration used for the complexes), and (c) positive controls, in which cells were exposed to different concentrations of the anticancer drug cisplatin.

Syntheses. *General Procedure for the Synthesis of Thiosemicarbazone Ligands (**L1** and **L2**).* The synthesis of ligands **L1** and **L2** was performed using the following adapted literature procedure.[54,55] The appropriate aldehyde (1 mol equiv) was dissolved in a hot toluene solution (20 mL) containing few drops of glacial acetic acid. An equimolar amount of the corresponding thiosemicarbazide (1 mol equiv) was added to the solution, and the reaction mixture was heated under reflux for 8 h. The solution was cooled to ambient temperature, and the TSC ligands were obtained as precipitate. After filtration the solid was washed several times with toluene and ether and dried under vacuum.

*N-(2-Hydroxy)-3-methoxybenzylidenethiosemicarbazide (**L1**).* White powder, yield: 87%. ^{1}H NMR (DMSO-d_6): δ 11.39 (s, 1H, NH), 9.17 (s, 1H, OH), 8.40 (s, 1H, CH═N), 8.10−7.88 (2s, 1H +1H, NH_2), 7.52 (d, 1H, J = 7.5 Hz, CH_{Ar}), 6.95 (d, 1H, J = 7.5 Hz, CH_{Ar}), 6.75 (t, 1H, J = 7.5 Hz, CH_{Ar}), 3.81 (s, 3H, OCH_3). ESI-MS ($C_9H_{11}N_3SO_2$, MeOH): m/z= 225 $[M + H]^+$.

*N-(2,3-Dihydroxybenzylidene)-3-phenylthiosemicarbazide (**L2**).* White powder, yield: 81%. ^{1}H NMR (DMSO-d_6): δ 11.76 (s, 1H, NH), 10.01−9.54 (2s, 1H+1H, OH), 9.01 (s, 1H, NH), 8.49 (s, 1H, CH═N), 7.56 (d, 2H, J = 7.5 Hz, CH_{Ar}), 7.49 (d, 2H, J = 8 Hz, CH_{Ar}), 7.34 (t, 2H, J = 7.5 Hz, CH_{Ar}), 7.17 (t, 1H, J = 7.5 Hz, CH_{Ar}), 6.81 (d, 1H, J = 8 Hz, CH_{Ar}), 6.64 (t, J = 8 Hz, CH_{Ar}). ESI-MS ($C_{14}H_{13}N_3SO_2$, MeOH): m/z= 287 $[M + H]^+$.

*General Procedure for the Metal Complexes Synthesis (**1**−**4**).* The TSC ligand (2 mol equiv) was dissolved in dry methanol (20 mL), and the solution was acidified with the addition of 1 drop of HCl 37%. $[(\eta^6\text{-}p\text{-cym})MCl_2]_2$ (1 mol equiv) was dissolved in 10 mL of dry dichloromethane, and the solution was added to the previous one. The reaction mixture was maintained under stirring at ambient temperature under nitrogen for 24 h. The volume was then reduced to half on the rotary evaporator, and diethyl ether was added until the precipitation of a solid occurred. The product was then collected by filtration and dried under vacuum.

*$[Os(\eta^6\text{-}p\text{-cym})Cl(L1)]Cl$ (**1**).* Orange powder, yield: 98%. Anal. Calcd for $C_{19}H_{25}Cl_2N_3O_2OsS$: C, 36.77; H, 4.06; N, 6.77. Found: C, 36.51; H, 4.56; N, 6.70. ^{1}H NMR (MeOD-d_4): δ 8.76 (s, 1H, CH═N), 7.86 (d, 1H, J = 8 Hz, CH_{Ar}), 7.25 (d, 1H, J = 8 Hz, CH_{Ar}), 7.01 (t, 1H, J = 8 Hz, CH_{Ar}), 5.87 (d, 1H, J = 5.5 Hz, $CH_{p\text{-cym}}$), 5.44 (d, 1H, J = 5.5 Hz, $CH_{p\text{-cym}}$), 5.31 (d, 1H, J = 5.5 Hz, $CH_{p\text{-cym}}$), 4.90 (d, 1H, J = 5.5 Hz, $CH_{p\text{-cym}}$), 3.99 (s, 3H, OCH_3), 2.54 (m, 1H, J = 7 Hz, $CH_{i\text{-prop}}$), 2.16 (s, 3H, CH_3), 1.20−1.11 (2d, 3H+3H, J = 7 Hz, $CH_{3i\text{-prop}}$). ESI-MS (positive ions, MeOH): m/z= 585 $[M - Cl]^+$. Crystals suitable for X-ray analysis were obtained by vapor diffusion of ether into a saturated methanol solution of the compound.

*$[Os(\eta^6\text{-}p\text{-cym})Cl(L2)]Cl$ (**2**).* Orange powder, yield: 72%. Anal. Calcd for $C_{24}H_{27}Cl_2N_3O_2OsS{\cdot}H_2O$: C, 41.14; H, 4.17; N, 6.00. Found: C,

DOI: 10.1021/acs.organomet.7b00875
Organometallics 2018, 37, 891−899

40.81; H, 4.16; N, 6.23. ^{1}H NMR (MeOD-d_4): δ 8.87 (s, 1H, CH═N), 7.75 (d, 1H, J = 7 Hz, CH_{Ar}), 7.48 (t, 2H, J = 7 Hz, CH_{Ar}), 7.43 (d, 2H, J = 7 Hz, CH_{Ar}), 7.35 (t, 1H, J = 7 Hz, CH_{Ar}), 7.08 (dd, 1H, J = 8 Hz, CH_{Ar}), 6.88 (t, 1H, J = 8 Hz, CH_{Ar}), 5.86 (d, 1H, J = 5.5 Hz, $CH_{p\text{-cym}}$), 5.49 (d, 1H, J = 5.5 Hz, $CH_{p\text{-cym}}$), 5.31 (d, 1H, J = 5.5 Hz, $CH_{p\text{-cym}}$), 4.93 (d, 1H, J = 5.5 Hz, $CH_{p\text{-cym}}$), 2.55 (m, 1H, J = 7 Hz, $CH_{i\text{-prop}}$), 1.21−1.13 (2d, 3H+3H, J = 7 Hz, $CH_{3i\text{-prop}}$). ESI-MS (positive ions, CH_3OH): m/z= 648 $[M - Cl]^+$. Crystals suitable for X-ray analysis were obtained by slow evaporation of a saturated acetone solution.

*[Ru(η^6-p-cym)Cl(L1)]Cl (**3**).* Red powder, yield: 78%. Anal. Calcd for $C_{19}H_{25}Cl_2N_3O_2RuS{\cdot}CH_3OH$: C, 42.63; H, 5.19; N, 7.46. Found: C, 41.92; H, 5.21; N, 7.34. ^{1}H NMR (MeOD-d_4): δ 8.79 (s, 1H, CH═N), 8.06 (d, 1H, J = 8 Hz, CH_{Ar}), 7.28 (d, 1H, J = 8 Hz, CH_{Ar}), 7.07 (t, 1H, J = 8 Hz, CH_{Ar}), 5.71 (d, 1H, J = 6 Hz, $CH_{p\text{-cym}}$), 5.17 (d, 1H, J = 6 Hz, $CH_{p\text{-cym}}$), 5.04 (d, 1H, J = 6 Hz, $CH_{p\text{-cym}}$), 4.00 (s, 3H, OCH_3), 2.64 (m, 1H, J = 7 Hz, $CH_{i\text{-prop}}$), 2.10 (s, 3H, CH_3), 1.20−1.14 (2d, 3H+3H, J = 7 Hz, $CH_{3i\text{-prop}}$). ESI-MS (positive ions, CH_3OH): m/z= 496 $[M - Cl]^+$. Crystals suitable for X-ray analysis were obtained by vapor diffusion of ether into a saturated methanol solution of the compound.

*[Ru(η^6-p-cym)Cl(L2)]Cl (**4**).* Red powder, yield: 87%. Anal. Calcd for $C_{24}H_{27}Cl_2N_3O_2RuS{\cdot}CH_3COCH_3$: C, 49.77; H, 5.10; N, 6.45. Found: C, 49.54; H, 5.23; N, 7.01. ^{1}H NMR (MeOD-d_4): δ 8.90 (s, 1H, CH═N), 7.95 (dd, 1H, J = 8 Hz, J' = 1 Hz, CH_{Ar}), 7.48 (t, 2H, J = 7.5 Hz, CH_{Ar}), 7.41 (d, 2H, J = 7.5 Hz, CH_{Ar}), 7.37 (d, 1H, J = 7 Hz, CH_{Ar}), 7.09 (td, 1H, J = 8 Hz, J' =1 Hz, CH_{Ar}), 6.94 (t, 1H, J = 7.5 Hz, CH_{Ar}), 5.86 (d, 1H, J = 5.5 Hz, $CH_{p\text{-cym}}$), 5.49 (d, 1H, J = 5.5 Hz, $CH_{p\text{-cym}}$), 5.31 (d, 1H, J = 5.5 Hz, $CH_{p\text{-cym}}$), 4.93 (d, 1H, J = 5.5 Hz, $CH_{p\text{-cym}}$), 2.55 (m, 1H, J = 7 Hz, $CH_{i\text{-prop}}$), 1.21−1.13 (2d, 3H+3H, J = 7 Hz, $CH_{3i\text{-prop}}$). ESI-MS (positive ions, CH_3OH): m/z= 558 $[M - Cl]^+$. Crystals suitable for X-ray analysis were obtained by slow evaporation of a saturated acetone solution of the compound.

X-ray Crystallography. Diffraction data were obtained on an Xcalibur Gemini diffractometer four-circle system with a Ruby CCD area detector using Mo Kα radiation. Absorption corrections were applied using ABSPACK.[69] The crystals were mounted on a glass fiber with Fromblin oil and kept at 150(2) K during data collection. Using Olex2,[70] the structure was solved with the ShelXT[71] structure solution program using Direct Methods and refined with the ShelXL refinement package using least-squares minimization.

NMR Spectroscopy. ^{1}H NMR spectra were obtained in 5 mm NMR precision tubes at 298 K on either Bruker DPX-300 or DPX-400 NMR spectrometers. ^{1}H NMR chemical shifts were internally referenced to residual protiated solvent for DMSO-d_6 (2.50 ppm), CD_3OD (3.31 ppm), D_2O (4.79 ppm), $(CD_3)_2CO$ (2.05 ppm). ^{1}H NMR spectra at variable temperature were obtained in 5 mm NMR precision tube on a Bruker AV-III 400 NMR spectrometer. NOESY spectra were obtained in 5 mm NMR precision tubes at 298 K on a Bruker DPX-500 NMR spectrometer. ^{1}H NMR peaks were internally referenced to CHD_2OD (3.31 ppm) for methanol-d_4 or 1,4-dioxane (3.66 ppm). All data processing was carried out using MestReNova 9.0.1.

Mass Spectrometry. Electrospray ionization mass spectra (ESI-MS) were obtained by preparing the sample in methanol using a Bruker Esquire 2000 ion trap spectrometer. Samples were prepared in methanol. The mass spectra were recorded with a scan range of m/z 50−500 for positive ions for **L1-L2** and m/z 400−1000 for positive ions for the complexes **1**−**4**.

UV−Vis Spectroscopy. UV−vis absorption spectra were recorded on a Cary 300 spectrometer using quartz cuvettes of 1 cm path-length (600 μL). The sample temperature was adjusted to 298 K by PTP1 Peltier temperature controller. Samples were prepared in methanol. Spectra were recorded from 200 to 600 nm. Data were processed with Microsoft Excel 14.3.6 Mac version.

■ ASSOCIATED CONTENT

Supporting Information

The Supporting Information is available free of charge on the ACS Publications website at DOI: 10.1021/acs.organomet.7b00875.

X-ray crystallographic data, ^{1}H-^{1}H 2D NMR NOESY and ^{1}H NMR spectra, UV−vis spectra, dose−response curves (PDF)

Accession Codes

CCDC 1584383−1584386 contain the supplementary crystallographic data for this paper. These data can be obtained free of charge via www.ccdc.cam.ac.uk/data_request/cif, or by emailing data_request@ccdc.cam.ac.uk, or by contacting The Cambridge Crystallographic Data Centre, 12 Union Road, Cambridge CB2 1EZ, UK; fax: +44 1223 336033.

■ AUTHOR INFORMATION

Corresponding Authors

*E-mail: P.J.Sadler@warwick.ac.uk. Phone: (+44) 024 7652 3818.

*E-mail: mauro.carcelli@unipr.it. Phone (+33) 0521 905427.

ORCID

Dominga Rogolino: 0000-0003-2295-5783

Peter J. Sadler: 0000-0001-9160-1941

Mauro Carcelli: 0000-0001-5888-4556

Notes

The authors declare no competing financial interest.

■ ACKNOWLEDGMENTS

We thank The Wellcome Trust (107691/Z/15/Z), EPSRC (EP/F034210/1) and the University of Warwick Development Trust for their support for this work. "Centro Interdipartimentale Misure Giuseppe Casnati" of the University of Parma is thanked for facilities.

■ REFERENCES

(1) Alagesan, M.; Sathyadevi, P.; Krishnamoorthy, P.; Bhuvanesh, N.; Dharmaraj, N. *Dalton Trans.* **2014**, *43*, 15829−15840.

(2) Yildirim, H.; Guler, E.; Yavuz, M.; Ozturk, N.; Yaman, P. K.; Subasi, E.; Sahin, E.; Timur, S. *Mater. Sci. Eng., C* **2014**, *44*, 1−8.

(3) Lobana, T. S.; Kumari, P.; Castineiras, A.; Butcher, R. J. *Polyhedron* **2009**, *253*, 977−1055.

(4) Rodríguez-Argüelles, M. C.; Mosquera-Vázquez, S.; Sanmartín-Matalobos, J.; García-Deibe, A. M.; Pelizzi, C.; Zani, F. *Polyhedron* **2010**, *29*, 864−870.

(5) Adams, M.; de Kock, C.; Smith, P. J.; Land, K. M.; Liu, N.; Hopper, M.; Hsiao, A.; Burgoyne, A. R.; Stringer, T.; Meyer, M.; Wiesner, L.; Chibale, K.; Smith, G. S. *Dalton Trans.* **2015**, *44*, 2456−2468.

(6) Beckford, F. A.; Leblanc, G.; Thessing, J.; Shaloski, M., Jr.; Frost, B. J.; Li, L.; Seeram, N. P. *Inorg. Chem. Commun.* **2009**, *12*, 1094−1098.

(7) Su, W.; Zhou, Q.; Huang, Y.; Huang, Q.; Huo, L.; Xiao, Q.; Huang, S.; Huang, C.; Chen, R.; Qian, Q.; Liu, L.; Li, P. *Appl. Organomet. Chem.* **2013**, *27*, 307−312.

(8) Chellan, P.; Land, K. M.; Shokar, A.; Au, A.; An, S. H.; Clavel, C. M.; Dyson, P. J.; de Kock, C.; Smith, P. J.; Chibale, K.; Smith, G. S. *Organometallics* **2012**, *31*, 5791−5799.

(9) Serda, M.; Kalinowski, D. S.; Rasko, N.; Potůčková, E.; Mrozek-Wilczkiewicz, A.; Musiol, R.; Małecki, J. G.; Sajewicz, M.; Ratuszna, A.; Muchowicz, A.; Gołąb, J.; Šimůnek, T.; Richardson, D. R.; Polanski, J. *PLoS One* **2014**, *9*, e110291.

(10) Lukmantara, A. Y.; Kalinowski, D. S.; Kumar, N.; Richardson, D. R. *Bioorg. Med. Chem. Lett.* **2013**, *23*, 967−974.
(11) Thota, S.; Vallala, S.; Yerra, R.; Barreiro, E. *Chin. Chem. Lett.* **2015**, *26*, 721−726.
(12) Stefani, C.; Jansson, P. J.; Gutierrez, E.; Bernhardt, P. V.; Richardson, D. R.; Kalinowski, D. S. *J. Med. Chem.* **2013**, *56*, 357−370.
(13) Agrawal, K. C.; Booth, B. A.; Moore, E. C.; Sartorelli, A. C. *J. Med. Chem.* **1972**, *15*, 1154−1158.
(14) Shao, J.; Zhou, B.; Di Bilio, A. J.; Zhu, L.; Wang, T.; Qi, C.; Shih, J.; Yen, Y. *Mol. Cancer Ther.* **2006**, *5*, 586−592.
(15) Zhu, L.; Zhou, B.; Chen, X.; Jiang, H.; Shao, J.; Yen, Y. *Biochem. Pharmacol.* **2009**, *78*, 1178−1185.
(16) Kovacevic, Z.; Chikhani, S.; Lovejoy, D. B.; Richardson, D. R. *Mol. Pharmacol.* **2011**, *80*, 598−609.
(17) Kovacevic, Z.; Sivagurunathan, S.; Mangs, H.; Chikhani, S.; Zhang, D.; Richardson, D. R. *Carcinogenesis* **2011**, *32*, 732−740.
(18) Bernhardt, P. V.; Sharpe, P. C.; Islam, M.; Lovejoy, D. B.; Kalinowski, D. S.; Richardson, D. R. *J. Med. Chem.* **2009**, *52*, 407−415.
(19) Richardson, D. R.; Sharpe, P. C.; Lovejoy, D. B.; Senaratne, D.; Kalinowski, D. S.; Islam, M.; Bernhardt, P. V. *J. Med. Chem.* **2006**, *49*, 6510−6521.
(20) Lovejoy, D. B.; Jansson, P. J.; Brunk, U. T.; Wong, J.; Ponka, P.; Richardson, D. R. *Cancer Res.* **2011**, *71*, 5871−5881.
(21) Su, W.; Qian, Q.; Li, P.; Lei, X.; Xiao, Q.; Huang, S.; Huang, C.; Cui, J. *Inorg. Chem.* **2013**, *52*, 12440−12449.
(22) Zeglis, B. M.; Divilov, V.; Lewis, J. S. *J. Med. Chem.* **2011**, *54*, 2391−2398.
(23) Barry, N. P. E.; Sadler, P. J. *ACS Nano* **2013**, *7*, 5654−5659.
(24) Beraldo, H.; Gambino, D. *Mini-Rev. Med. Chem.* **2004**, *4*, 31−39.
(25) Liu, Y.-H.; Li, A.; Shao, J.; Xie, C.-Z.; Song, X.-Q.; Bao, W.-G.; Xu, J.-Y. *Dalton Trans.* **2016**, *45*, 8036−8049.
(26) Kowol, C. R.; Trondl, R.; Heffeter, P.; Arion, V. B.; Jakupec, M. A.; Roller, A.; Galanski, M.; Berger, W.; Keppler, B. K. *J. Med. Chem.* **2009**, *52*, 5032−5043.
(27) Kalaivani, P.; Prabhakaran, R.; Poornima, P.; Dallemer, F.; Vijayalakshmi, K.; Padma, V. V.; Natarajan, K. *Organometallics* **2012**, *31*, 8323−8332.
(28) Dilruba, S.; Kalayda, G. V. *Cancer Chemother. Pharmacol.* **2016**, *77*, 1103−1124.
(29) Clavel, C. M.; Păunescu, E.; Nowak-Sliwinska, P.; Griffioen, A. W.; Scopelliti, R.; Dyson, P. J. *J. Med. Chem.* **2014**, *57*, 3546−3558.
(30) Wong, E.; Giandomenico, C. M. *Chem. Rev.* **1999**, *99*, 2451−2466.
(31) Hartinger, C. G.; Jakupec, M. A.; Zorbas-Seifried, S.; Groessl, M.; Egger, A.; Berger, W.; Zorbas, H.; Dyson, P. J.; Keppler, B. K. *Chem. Biodiversity* **2008**, *5*, 2140−2155.
(32) Perekalin, D. S.; Molotkov, A. P.; Nelyubina, Y. V.; Anisimova, N. Y.; Kudinov, A. R. *Inorg. Chim. Acta* **2014**, *409*, 390−393.
(33) Ang, W. H.; Daldini, E.; Scolaro, C.; Scopelliti, R.; Juillerat-Jeannerat, L.; Dyson, P. *Inorg. Chem.* **2006**, *45*, 9006−9013.
(34) Clarke, M. J.; Zhu, F.; Frasca, D. R. *Chem. Rev.* **1999**, *99*, 2511−2533.
(35) Romero-Canelón, I.; Salassa, L.; Sadler, P. J. *J. Med. Chem.* **2013**, *56*, 1291−1300.
(36) Yan, Y. K.; Melchart, M.; Habtemariam, A.; Sadler, P. J. *Chem. Commun.* **2005**, 4764−4776.
(37) Chelopo, M. P.; Pawar, S. A.; Sokhela, M. K.; Govender, T.; Kruger, H. G.; Maguire, G. E. M. *Eur. J. Med. Chem.* **2013**, *66*, 407−414.
(38) Smith, G. S.; Therrien, B. *Dalton Trans.* **2011**, *40*, 10793−10800.
(39) van Rijt, S. H.; Sadler, P. J. *Drug Discovery Today* **2009**, *14*, 1089−1097.
(40) Dempsey, J. L.; Winkler, J. R.; Gray, H. B. *Dalton Trans.* **2011**, *40*, 10633−10636.
(41) Fu, Y.; Habtemariam, A.; Pizarro, A. M.; van Rijt, S. H.; Healey, D. J.; Cooper, P. A.; Shnyder, S. D.; Clarkson, G. J.; Sadler, P. J. *J. Med. Chem.* **2010**, *53*, 8192−8196.
(42) Shnyder, S. D.; Fu, Y.; Habtemariam, A.; van Rijt, S. H.; Cooper, P. A.; Loadman, P. M.; Sadler, P. J. *MedChemComm* **2011**, *2*, 666−668.
(43) Hanif, M.; Babak, M. V.; Hartinger, C. G. *Drug Discovery Today* **2014**, *19*, 1640−1648.
(44) Suntharalingam, K.; Lin, W.; Johnstone, T. C.; Bruno, P. M.; Zheng, Y.-R.; Hemann, M. T.; Lippard, S. J. *J. Am. Chem. Soc.* **2014**, *136*, 14413−14416.
(45) Büchel, G. E.; Kossatz, S.; Sadique, A.; Rapta, P.; Zalibera, M.; Bucinsky, L.; Komorovsky, S.; Telser, J.; Eppinger, J.; Reiner, T.; Arion, V. B. *Dalton Trans.* **2017**, *46*, 11925−11941.
(46) Riedl, C. A.; Flocke, L. S.; Hejl, M.; Roller, A.; Klose, M. H. M.; Jakupec, M. A.; Kandioller, W.; Keppler, B. K. *Inorg. Chem.* **2017**, *56*, 528−541.
(47) Fish, R. H.; Jaouen, G. *Organometallics* **2003**, *22*, 2166−2177.
(48) Hung, Y.; Kung, W. J.; Taube, H. *Inorg. Chem.* **1981**, *20*, 457−463.
(49) Peacock, A. F. A.; Habtemariam, A.; Fernández, R.; Walland, V.; Fabbiani, F. P. A.; Parsons, S.; Aird, R. E.; Jodrell, D. I.; Sadler, P. J. *J. Am. Chem. Soc.* **2006**, *128*, 1739−1748.
(50) Stebler-Roethlisberger, M.; Hummel, W.; Pittet, P. A.; Buergi, H. B.; Ludi, A.; Merbach, A. E. *Inorg. Chem.* **1988**, *27*, 1358−1363.
(51) Brumaghim, J. L.; Priepot, J. G.; Girolami, G. S. *Organometallics* **1999**, *18*, 2139−2144.
(52) Wang, F.; Chen, H.; Parsons, S.; Oswald, I. D. H.; Davidson, J. E.; Sadler, P. J. *Chem. - Eur. J.* **2003**, *9*, 5810−5820.
(53) Chen, H.; Parkinson, J. A.; Nováková, O.; Bella, J.; Wang, F.; Dawson, A.; Gould, R.; Parsons, S.; Brabec, V.; Sadler, P. J. *Proc. Natl. Acad. Sci. U. S. A.* **2003**, *100*, 14623−14628.
(54) Đilović, I.; Rubčić, M.; Vrdoljak, V.; Pavelić, S. K.; Kralj, M.; Piantanida, I.; Cindrić, M. *Bioorg. Med. Chem.* **2008**, *16*, 5189−5198.
(55) Rogolino, D.; Bacchi, A.; De Luca, L.; Rispoli, G.; Sechi, M.; Stevaert, A.; Naesens, L.; Carcelli, M. *JBIC, J. Biol. Inorg. Chem.* **2015**, *20*, 1109−1121.
(56) Beckford, F.; Dourth, D.; Shaloski, M., Jr.; Didion, J.; Thessing, J.; Woods, J.; Crowell, V.; Gerasimchuk, N.; Gonzalez-Sarrías, A.; Seeram, N. P. *J. Inorg. Biochem.* **2011**, *105*, 1019−1029.
(57) Tan, K. W.; Farina, Y.; Ng, C. H.; Maah, M. J.; Ng, S. W. *Acta Crystallogr., Sect. E: Struct. Rep. Online* **2008**, *64*, o1035.
(58) Fun, H.-K.; Kia, R.; D'Silva, E. D.; Patil, P. S.; Dharmaprakash, S. M. *Acta Crystallogr., Sect. E: Struct. Rep. Online* **2008**, *64*, o2274.
(59) de Oliveira, A. B.; Feitosa, B. R. S.; Näther, C.; Jess, I. *Acta Crystallogr., Sect. E: Struct. Rep. Online* **2013**, *69*, o1861.
(60) Schmid, W. F.; John, R. O.; Arion, V. B.; Jakupec, M. A.; Keppler, B. K. *Organometallics* **2007**, *26*, 6643−6652.
(61) Belicchi Ferrari, M.; Capacchi, S.; Pelosi, G.; Reffo, G.; Tarasconi, P.; Albertini, R.; Pinelli, S.; Lunghi, P. *Inorg. Chim. Acta* **1999**, *286*, 134−141.
(62) Palla, G.; Predieri, G.; Domiano, P.; Vignali, C.; Turner, W. *Tetrahedron* **1986**, *42*, 3649−3654.
(63) Su, W.; Tang, Z.; Li, P.; Wang, G.; Xiao, Q.; Li, Y.; Huang, S.; Gu, Y.; Lai, Z.; Zhang, Y. *Dalton Trans.* **2016**, *45*, 19329−19340.
(64) Khalilian, M. H.; Mirzaei, S.; Taherpour, A. *New J. Chem.* **2015**, *39*, 9313−9324.
(65) Su, W.; Peng, B.; Li, P.; Xiao, Q.; Huang, S.; Gu, Y.; Lai, Z. *Appl. Organomet. Chem.* **2017**, *31*, 1−7.
(66) Patra, M.; Joshi, T.; Pierroz, V.; Ingram, K.; Kaiser, M.; Ferrari, S.; Spingler, B.; Keiser, J.; Gasser, G. *Chem. - Eur. J.* **2013**, *19*, 14768−14772.
(67) Gourdier, I.; Del Rio, M.; Crabbe, L.; Candeil, L.; Copois, V.; Ychou, M.; Auffray, C.; Martineau, P.; Mechti, N.; Pommier, Y.; Pau, B. *FEBS Lett.* **2002**, *529*, 232−236.
(68) Bennett, M. A.; Smith, A. K. *J. Chem. Soc., Dalton Trans.* **1974**, 233−241.
(69) *CrysAlis PRO*; Oxford Diffraction Ltd.: Abington, Oxfordshire, U.K., 2007.
(70) Dolomanov, O. V.; Bourhis, L. J.; Gildea, R. J.; Howard, J. A. K.; Puschmann, H. *J. Appl. Crystallogr.* **2009**, *42*, 339−341.
(71) Sheldrick, G. M. *SHELXL-97*; University of Göttingen: Göttingen, Germany, 1997.

DOI: 10.1021/acs.organomet.7b00875
Organometallics 2018, 37, 891−899